UNIVERSITY^{OF} BIRMINGHAM University of Birmingham Research at Birmingham

Objective Uniaxial Identification of Transition Points in Non-Linear Materials

Freij, Jenny M; Burton, Hanna; Espino, Daniel

DOI: 10.1007/s13239-018-00395-x

License: Other (please specify with Rights Statement)

Document Version Peer reviewed version

Citation for published version (Harvard):

Freij, JM, Burton, H & Espino, D 2018, Objective Uniaxial Identification of Transition Points in Non-Linear Materials: Sample Application to Porcine Coronary Arteries and the Dependency of Their Pre- and Post-Transitional Moduli with Position', *Cardiovascular Engineering and Technology*. https://doi.org/10.1007/s13239-018-00395-x

Link to publication on Research at Birmingham portal

Publisher Rights Statement:

This is the version of the above work as accepted for publication. Final version of record available at: https://doi.org/10.1007/s13239-018-00395-x

General rights

Unless a licence is specified above, all rights (including copyright and moral rights) in this document are retained by the authors and/or the copyright holders. The express permission of the copyright holder must be obtained for any use of this material other than for purposes permitted by law.

•Users may freely distribute the URL that is used to identify this publication.

•Users may download and/or print one copy of the publication from the University of Birmingham research portal for the purpose of private study or non-commercial research.

•User may use extracts from the document in line with the concept of 'fair dealing' under the Copyright, Designs and Patents Act 1988 (?) •Users may not further distribute the material nor use it for the purposes of commercial gain.

Where a licence is displayed above, please note the terms and conditions of the licence govern your use of this document.

When citing, please reference the published version.

Take down policy

While the University of Birmingham exercises care and attention in making items available there are rare occasions when an item has been uploaded in error or has been deemed to be commercially or otherwise sensitive.

If you believe that this is the case for this document, please contact UBIRA@lists.bham.ac.uk providing details and we will remove access to the work immediately and investigate.

1	Objective uniaxial identification of transition points in non-linear
2	materials: sample application to porcine coronary arteries and the
3	dependency of their pre- and post-transitional moduli with position.
4	
5	Jenny M. Freij (<u>freij.jenny@gmail.com</u>)
6	Hanna E. Burton (h.e.burton@bham.ac.uk)
7	Daniel M. Espino* (d.m.espino@bham.ac.uk)
8	
9	Department of Mechanical Engineering, University of Birmingham, Birmingham, B15 2TT,
10	United Kingdom
11	*Corresponding author:
12	Daniel M Espino
13	Department of Mechanical Engineering,
14	University of Birmingham
15	Birmingham
16	United Kingdom, B15 2TT
17	Tel.: +44 (0) 121 414 7355
18	Fax: +44 (0) 121 414 3958
19	Email address: d.m.espino@bham.ac.uk
20	
21	ACKNOWLEDGEMENTS
22	The authors would like to thank the Engineering and Physical Sciences Research Council for
23	the studentship for HEB [EP/M114612B]. The equipment used in this study was funded by
24	Arthritis Research UK [H0671].

1 Abstract

2 **Purpose:** This study aimed to develop an objective method for the elastic characterisation of 3 pre- and post-transitional moduli of left anterior descending (LAD) porcine coronary arteries. 4 Methods: Eight coronary arteries were divided into proximal, middle and distal test 5 specimens. Specimens underwent uniaxial extension up to 3 mm. Force-displacement 6 measurements were used to determine the induced true stress and stretch for each specimen. 7 A local maximum of the stretch-true stress data was used to identify a transition point. Pre-8 and post-transitional moduli were calculated up to and from this point, respectively. 9 **Results**: The mean pre-transitional moduli for all specimens was 0.76 MPa, as compared to 10 4.86 MPa for the post-transitional moduli. However, proximal post-transitional moduli were 11 significantly greater than that of middle and distal test specimens (p < 0.05). 12 **Conclusion**: post-transitional uniaxial properties of the LAD are dependent on location along 13 the artery. Further, it is feasible to objectively identify a transition point between pre- and 14 post-transitional moduli. 15

16 Keywords: Biomechanical Testing/ Analysis, Connective tissues, Coronary artery,

17 Mechanical properties, Young's modulus.

1 Background

Coronary heart disease is the leading cause of death worldwide [1]. Characterising the
mechanical properties of coronary arteries is important in order to determine stress and strain
on the arterial wall [2] and is thus vital for clinical treatments of arterial diseases, designs of
vascular implants (e.g. stents and grafts) as well as for tissue engineering [3].

6 The coronary arteries are the first arterial branches of the aorta [4] with the main 7 function of distributing oxygen at a high rate to the myocardium [5]. One of the two major 8 branches of coronary circulation is the left coronary artery [6] of which the left anterior 9 descending coronary artery (LAD) is of central importance [3]. The left coronary artery and 10 its branches supply a majority of the oxygenated blood to the ventricular myocardium, as 11 well as to the left atrium, left atrial appendage, pulmonary arteries and aortic root [5]. 12 Coronary artery disease leads to chronic narrowing of the vessels or impaired vascular 13 function which in turn can lead to cardiac hypoxia and impaired contractile function as well 14 as increase the risk for a myocardial infarction [6].

15 Mechanical testing has been performed on both human [5,7-9], and porcine [2,9,10] 16 coronary arteries. Porcine hearts are often chosen for their anatomical similarity to human 17 hearts [8]. Uniaxial testing is a commonly chosen method for testing of coronary arteries 18 [3,8-10], with elastic material parameters often used in computational models [10-12]. 19 However, a repeatable but objective measure of the pre- and post-transitional moduli 20 following stress-stretch uniaxial testing is not currently available. There is the potential to use differences in post-transitional moduli to distinguish between healthy and diseased arteries 21 22 [7]; with potential for clinical translation via elastography. Further, variations in these moduli 23 along the length of the artery are unknown.

The aim of this study was to objectively measure the uniaxial behaviour of the left anterior descending coronary arteries of porcine hearts. Therefore, a method to identify the

pre- and post-transitional moduli of arteries following uniaxial tests has been trialled. The
 methodology has been applied to proximal, middle and distal LAD coronary artery samples.
 3

4 Methods

5 Specimens

6 Eight coronary arteries were obtained from eight porcine hearts. The porcine hearts were 7 delivered from a supplier (Fresh Tissue Supplies, Horsham, UK) who froze the hearts when 8 excised and delivered them frozen and sealed. When delivered to the laboratory, the hearts 9 were individually wrapped in tissue paper, soaked in Ringer's solution and then stored 10 at -40 °C in heat sealed bags. This followed protocols from previous studies involving 11 porcine hearts [13-17]. Porcine hearts were thawed overnight at 4 °C, after which the LAD 12 coronary artery was dissected from intact hearts. Each LAD coronary artery's length, width 13 and thickness was measured before and after being divided into proximal, middle and distal 14 test specimens, each 20.58 ± 0.75 mm in length (Figure 1; Table 1). Specimens underwent a 15 second freeze-thaw cycle ahead of uniaxial testing.

16

17 Uniaxial testing

18 Test specimens were held in place using grips lined with emery paper. A piece of P400 emery 19 paper with two rougher rectangular pieces of P60 emery paper, glued on using Araldite® 20 Rapid (Huntsman Corporation, Texas, USA), was folded around the sample. Grips were 21 attached to a Bose 3200 materials testing machine operated by WinTest software (Bose 22 Corporation, ElectroForce Systems Group, Minnesota, USA). Each test specimen had a 23 gauge length of 4.57 ± 0.75 mm. A thin piece of hydrated tissue paper was wrapped around 24 the sample and re-hydrated with Ringer's solution between each cycle in order to avoid 25 dehydration, as often performed for other soft connective tissues [13,18].

Each sample underwent ten cycles of uniaxial testing, for each cycle it was stretched to a longitudinal displacement of 3 mm at a rate of 0.5 mm/s (i.e. tested axially), consistent with the longitudinal displacement of the left coronary artery [19,20] which ranges from 0.5 mm to 6.5 mm for the LAD [19]. Specimens were not tested to failure, as specimens were also used as part of a separate study [21]. Force-displacement data from the tenth, and final, cycle was used to calculate the pre- and post- transitional moduli (Figure 2). The first nine cycles were used as preconditioning cycles, which coronary arteries require [2,3,10,22].

8

9 Pre- and post-transitional modulus

10 Coronary arteries typically display a 'J-shaped' curve during uniaxial tests [12,23], by 11 convention plotted as true stress, σ , over stretch, λ , [2,3,12,23,24] where λ is defined by 12 equation 1 in terms of the actual length, *l*, and the initial length, *L* [10,23]. The initial length 13 corresponded to the gauge length (see *Unaxial testing*, above) was used for calculations. 14 Coronary arteries are considered to be incompressible [7,11,25], so equation 2 is used to 15 calculate the actual cross-sectional area, a, in relation to the initial cross-sectional area, A. 16 Therefore, σ can be calculated using equation 3 based on the measured load, P, during testing 17 [23].

18 $\lambda = \frac{l}{L} \tag{1}$

19
$$a = \frac{A}{\lambda}$$
 (2)

- 20 $\sigma = \frac{P}{a}$
- The stress-stretch curve of coronary arteries contain what is commonly termed as a toe and a linear region [10,26,27] (Figure 3). The stress-strain gradient within these toe and linear regions are defined as the pre- and post-transitional moduli, respectively. For this study, a critical point has been identified with corresponding stress, σ_C , and stretch λ_C . This critical point, *C* in Figure 3, was defined by identifying the critical point closest to the origin (for λ , σ

(3)

1 > 0) of the estimated polynomial regression line of the data plotted as the stretch over true 2 stress. A third-degree polynomial regression line has been used. This is because it was the lowest degree polynomial which led to a suitable goodness of fit ($R^2 = 85.65 \pm 9.19$ %). 3 4 Further, it was the only regression trendline which consistently displayed an identifiable local 5 maximum at the transition point. This local maximum was identifiable when the data was plotted as the stretch over true stress (Figure 3). Thus, this is an essential part of this method; 6 7 the use of lower order polynomials, for example, did not always lead to such an identifiable 8 point. The critical point stretch, λ_C , was used to identify a corresponding stretch (up to two 9 significant figures) on the actual experimental data which had been plotted. The result was a 10 transition stretch, λ_T . λ_T is necessary because λ_C does not necessarily match a data point on the 11 stress-stretch curve; λ_T is identified as the nearest data stretch point to λ_C . The transition 12 stretch, together with the corresponding transition true stress, σ_T , formed the transition point 13 (λ_T, σ_T) , point T in Figure 3. In essence, T is the mapping of C from the polynomial regression 14 line on to the experimental data. Subsequently, the pre- and post-transitional moduli were 15 calculated using point T as an end and start point for each, respectively. 16 17 Statistical analysis 18 The pre- and post-transitional moduli were analysed with respect to the LAD geometry. 19 Width and thickness of the samples were compared to the distance from the bifurcation, the 20 post-transitional modulus was compared to the width of the samples. Regression analysis was

21 performed with SigmaPlot (v12.0, Systat Software Inc., USA). Minitab (v17, Minitab Inc.,

USA) was used to assess statistical significance for one-way ANOVA (p < 0.05) between the

23 geometry of the proximal, middle and distal test specimens. Statistically significant

24 differences (p < 0.05) were also analysed between matched pre- and post-transitional moduli,

25 the storage and loss moduli using a paired *t*-test.

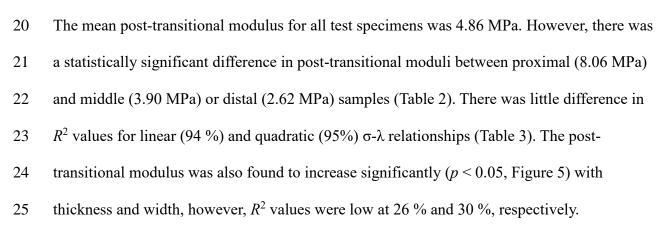
1 **Results**

The proximal, middle and distal samples had a mean width of 8.66 ± 1.03 mm, 6.90 ± 0.85 mm and 5.62 ± 0.63 mm (Table 1), respectively, and decreased significantly along the distance from the bifurcation (p < 0.05, $R^2 = 70.91$ %; Figure 4). The thickness of the proximal, middle and distal pieces were 0.49 ± 0.08 mm, 0.34 ± 0.06 mm and 0.29 ± 0.10 mm (Table 1), respectively, again decreasing significantly along the distance from the bifurcation (p < 0.05, $R^2 = 53.15$ %; Figure 4).

8 There was a statistically significant difference between pre- and post- transitional 9 moduli (Table 2). The average pre-transitional modulus ranged from 0.67 MPa for proximal 10 samples to 0.85 MPa for the distal samples; whereas, post-transitional moduli ranged from 11 2.62 MPa (distal) to 8.06 MPa (proximal). However, there was no statistically significant 12 difference between the stretch at which the transition point occurred for the proximal, middle 13 or distal samples. The average transition point occurred at $\lambda = 1.53 \pm 0.11$.

There was no significant difference between the pre-transitional moduli at different distances from the bifurcation (Table 2). The overall mean pre-transitional modulus was 0.76 ± 0.38 MPa. While a linear relationship was used to calculate this modulus, regression analysis shows that a quadratic fit (equation 4) provided a better fit for the data (Table 3). Constants from equation 4 for proximal, middle and distal samples are provided in Table 4.

19 $\sigma = \alpha \lambda^2 - \beta \lambda + \gamma \tag{4}$



1 Discussion

An objective method has been trialled to measure the pre- and post-transitional moduli for
proximal, middle and distal samples of the LAD coronary artery. The post-transitional
modulus varied across the length of the coronary artery and with the thickness of the LAD.
Unsurprisingly, there is a significant difference between the pre- and post-transitional moduli
of the LAD coronary artery. More importantly it was feasible to identify a transition point,
mathematically, to distinguish between pre- and post- transitional components of the true
stress-stretch curve.

9 The proximal post-transitional moduli from this study are consistent with the range of values available in literature, ranging from around 1.5 MPa [7] up to 10 MPa [10]. However, 10 11 the identification of the point from where this post-transitional region starts is vaguely 12 defined in previous studies [7,10]. Lower values of around 0.1 MPa have also been reported 13 in the literature [12,28]. However, such findings are based on biaxial tests and there are 14 difficulties in comparing between uniaxial and biaxial testing methodologies. Thus, although 15 the sample size used in this study could be considered low, the results obtained in our study 16 are consistent with available literature. Further our sample size exceeds that of other studies 17 in literature [29].

The method used to calculate and identify the pre- and post-transitional modulus, although novel, is based on there being an identifiable transition point between the pre- and post-transition of a stretch-stress curve of a coronary artery [23]. Considering the advantages of using a linear fit compared to a quadratic one in determining a pre- and post-transitional modulus, the use of a linear fit is thus considered of greater value. For example, implementation of a single pre- and/or post-transitional modulus simplifies the implementation in using computational models [30, 31]. However, it is noted that this may

introduce some limitations in terms of the pre-transitional modulus which is best represented
 by a quadratic σ-λ relationship.

9

3 The lumen diameter of LAD has been previously documented. Dodge *et al.* [32] and 4 Zhang et al. [33] observed the proximal and distal lumen diameter of human LAD coronary 5 artery to be 3.7 mm and 3.92 mm as well as 1.9 mm and 2.10 mm, respectively. Leung et 6 al.[34] measured the proximal human LAD lumen diameter to vary between 3.30-3.88 mm 7 and Guo et al. [35] found the inner lumen diameter of porcine LAD to vary between 2.19 mm 8 to 0.02 mm. During this study, the width of the LAD was measured when the specimen had 9 been cut open to resemble a rectangular specimen. Thus, the measured widths, w, from our 10 current study is a measure of the inner circumference of the artery. Assuming a circular cross-11 section, means that the outer diameter, d_o , measured in other studies would be approximately 12 equivalent to

13

$$d_o = \frac{w}{\pi} + 2t \tag{6}$$

14 here, t is the wall thickness. Thus, outer diameters for proximal, middle and distal samples 15 were 3.7 mm, 2.9 mm and 2.4 mm, respectively. Although the measured width of the 16 proximal section of the LAD in this study are consistent with those by Dodge et al. [32] and 17 Leung et al. [34] other comparisons are hard to make since the location of the distal section is 18 not always clear [36]. Measurements might also vary between human [33] and porcine 19 specimens. Geometrical considerations are important because our study found that post-20 transitional moduli decreased with LAD thickness and, thus, along the artery. 21 A limitation of this study is that samples have undergone freeze-thaw cycles. Briefly, 22 while freeze-thaw cycles might influence tissue mechanics to some extent, it is the method of

freezing which is critical [37, 38, 39]; as discussed elsewhere in more detail [21].

24 Microscopic assessment of coronary arteries using the freeze-thaw protocols employed in this

study have found limited effect on their structure [40]. Ultimately, the agreement of our data

1 with literature suggests that it has not impaired the mechanics of the tissues assessed. 2 Furthermore, as the overall stress-strain trend has not been altered by this process, it does not 3 limit the assessment of an objective method for identifying a transition point. Such a 4 transition point has potential uses clinically, in terms of distinguishing between pre- and post-5 transitional moduli. These moduli can be useful on their own in terms of enabling distinction 6 between healthy and diseased arteries [7] with potential applications to magnetic resonance 7 elastography [41] for diagnosis. Alternatively, they may enable the identification of linear 8 regions (i.e. post-transitional) for more advanced characterisation, such as dynamic 9 viscoelasticity of arteries [21], heart valves [42], and other tissues, replacement materials [43, 10 44] and/or chemically natural tissues [45]. Ahead implementation on a wide range of 11 materials, the authors would suggest that any test data used is consistent with existing 12 recommendations for test data to be suitable for characterisation, e.g. [46]. This is because 13 any characterisation method will be sensitive to the range of input data, and their spacing, as 14 the parameters of acquisition/sampling can disproportionately biasing subsequent fits 15 (altering subsequent coefficients determined through characterisation).

16

17 Conclusion

18 It is feasible to identify a transition point from a pre- to a post-transitional modulus of soft 19 connective tissues. Using this objective method, the post-transitional modulus of porcine left 20 anterior descending coronary arteries was found to decrease along its proximal-distal length. 21

- 22
- 23
- 24
- 25

1 Declarations

2 The authors declare that they have no conflict of interest;

3

4 Authors' contributions

5 JMF participated in the study's design, performed mechanical testing and drafted the initial

6 manuscript. HEB conceived the study, participated in its design, and edited the manuscript.

7 DME conceived the study, participated in its design, and edited the manuscript. All authors

8 read and approved the final manuscript.

9

10 Animal studies

11 No animals were sacrificed specifically for this study. Porcine hearts were supplied by Fresh

12 Tissue Supplies (Horsham, UK). Ethical approval was granted for this study by the

13 University of Birmingham Research Support Group, [ERN_15-0032].

1	Referen	ces

- Mackay J, Mensah GA. The Atlas of Heart Disease and Stroke. Geneva: World Health
 Organization; 2004.
- Wang C, Garcia M, Lu X, Lanir Y, Kassab GS. Three-dimensional mechanical
 properties of porcine coronary arteries: A validated two-layer model. Am J Physiol
 Heart Circ Physiol. 2006; 291:H1200-H1209.
- Holzapfel GA, Sommer G, Gasser CT, Regitnig P. Determination of layer-specific
 mechanical properties of human coronary arteries with nonatherosclerotic intimal
 thickening and related constitutive modeling. Am J Physiol Heart Circ Physiol. 2005;
- 10 289:H2048-H2058.
- Townsend Jr CM, Beauchamp RD, Evers BM, Mattox KL. Sabiston Textbook of
 Surgery. 19th ed. Philadelphia: Elsevier; 2012.
- 13 5. Katz AM. Physiology of the Heart. 5th ed. Philadelphia: Lippincott Williams &
 Wilkins; 2010.
- 15 6. Klabunde R. Cardiovascular Physiology Concepts. 2nd ed. Philadelphia: Lippincott
 Williams & Wilkins; 2011.
- Karimi A, Navidbakhsh M, Shojaei A, Faghihi S. Measurement of the uniaxial
 mechanical properties of healthy and atherosclerotic human coronary arteries. Mater
 Sci Eng C Mater Biol Appl. 2013; 33:2550-2554.
- Ozolanta I, Tetere G, Purinya B, Kasyanov V. Changes in the mechanical properties,
 biochemical contents and wall structure of the human coronary arteries with age and
 sex. Med Eng Phys. 1998; 20:523-533.
- Van Andel CJ, Pistecky PV, Borst C. Mechanical properties of porcine and human
 arteries: Implications for coronary anastomotic connectors. Ann Thorac Surg. 2003;
 76:58-64.

1	10.	Lally C, Reid A, Prendergast P. Elastic behavior of porcine coronary artery tissue under
2		uniaxial and equibiaxial tension. Ann Biomed Eng. 2004; 32:1355-1364.
3	11.	Holzapfel GA, Gasser TC, Stadler M. A structural model for the viscoelastic behavior
4		of arterial walls: continuum formulation and finite element analysis. Eur J Mech A
5		Solid. 2002; 21:441-463.
6	12.	Kural MH, Cai M, Tang D, Gwyther T, Zheng J, Billiar KL. Planar biaxial
7		characterization of diseased human coronary and carotid arteries for computational
8		modeling. J Biomech. 2012; 45:790-798.
9	13.	Wilcox AG, Buchan KG, Espino DM. Frequency and diameter dependent viscoelastic
10		properties of mitral valve chordae tendineae. J Mech Behav Biomed Mater. 2014;
11		30:186-195.
12	14.	Espino DM, Hukins DWL, Shepherd DET, Watson MA, Buchan KG. Determination of
13		the pressure required to cause mitral valve failure. Med Eng Phys. 2006; 28:36-41.
14	15.	Espino DM, Shepherd DET, Buchan KG. Effect of mitral valve geometry on valve
15		competence. Heart Vessels. 2007; 22:109-115.
16	16.	Millard L, Espino DM, Shepherd DET, Hukins DWL, Buchan KG. Mechanical
17		properties of chordae tendineae of the mitral heart valve: Young's modulus, structural
18		stiffness, and effects of aging. J Mech Med Biol. 2011; 11:221-230.
19	17.	Espino DM, Shepherd DET, Hukins DWL, Buchan KG. The role of chordae tendineae
20		in mitral valve competence. J Heart Valve Dis. 2005; 14:603-609.
21	18.	Öhman C, Baleani M, Viceconti M. Repeatability of experimental procedures to
22		determine mechanical behaviour of ligaments. Acta Bioeng Biomech. 2009; 11:19-23.
23	19.	Arbab-Zadeh A, DeMaria AN, Penny WF, Russo RJ, Kimura BJ, Bhargava V. Axial
24		movement of the intravascular ultrasound probe during the cardiac cycle: implications

1		for three-dimensional reconstruction and measurements of coronary dimensions. Am
2		Heart J. 1999; 138:865-872.
3	20.	Konta T, Hugh J, Bett N. Patterns of coronary artery movement and the development of
4		coronary atherosclerosis. Circulation. 2003; 67:846-850.
5	21.	Burton HE, Freij JM, Espino DM. Dynamic viscoelasticity and surface properties of
6		porcine left anterior descending coronary arteries. Cardiovasc Eng Technol. 2017; 8:41-
7		56.
8	22.	Humphrey JD. Cardiovascular solid mechanics: cells, tissues, and organs. New York:
9		Springer; 2002.
10	23.	Claes E, Atienza J, Guinea G, Rojo F, Bernal J, Revuelta J, et al. Mechanical properties
11		of human coronary arteries. Engineering in Medicine and Biology Society (EMBC).
12		2010 Annual International Conference of the IEEE: IEEE. 2010; pp. 3792-3795.
13	24.	Holzapfel GA, Ogden RW. Constitutive modelling of arteries. Proc R Soc A Math Phys
14		Eng Sci. 2010; 466:1551-1597.
15	25.	Holzapfel GA. Biomechanics of soft tissue. In: Lemaitre J (ed) The Handbook of
16		Materials Behavior Models: Nonlinear Models and Properties. France: Academic Press;
17		2010.
18	26.	Freed AD, Doehring TC. Elastic model for crimped collagen fibrils. J Biomech Eng.
19		2005; 127:587-593.
20	27.	Venkatasubramanian RT, Grassl ED, Barocas VH, Lafontaine D, Bischof JC. Effects of
21		freezing and cryopreservation on the mechanical properties of arteries. Ann Biomed
22		Eng. 2006; 34:823-832.
23	28.	Lu X, Pandit A, Kassab GS. Biaxial incremental homeostatic elastic moduli of coronary
24		artery: two-layer model. Am J Physiol Heart Circ Physiol. 2004; 287:H1663-H1669.

1	29. Khoffi F, Heim F. Private mechanical degradation of biological heart valve tissue induced
2	by low diameter crimping: an early assessment. J Mech Behav Biomed Mater. 2015;
3	44: 71-75.
4	30. Espino DM, Shepherd DET, Hukins DWL. Evaluation of a transient, simultaneous,
5	arbitrary Lagrange–Euler based multi-physics method for simulating the mitral heart
6	valve. Comput Methods Biomech Biomed Eng. 2014; 17:450-458.
7	31. Espino DM, Shepherd DET, Hukins DWL. Development of a transient large strain
8	contact method for biological heart valve simulations. Comput Methods Biomech
9	Biomed Eng. 2013; 16:413-424.
10	32. Dodge J, Brown BG, Bolson EL, Dodge HT. Lumen diameter of normal human
11	coronary arteries. Influence of age, sex, anatomic variation, and left ventricular
12	hypertrophy or dilation. Circulation. 1992; 86:232-246.
13	33. Zhang L, Xu D, Liu X, Wu XS, Ying YN, Dong Z., et al. Coronary artery lumen diameter
14	and bifurcation angle derived from CT coronary angiographic image in healthy people.
15	Chinese J Cardiol. 2011; 39:1117-1123.
16	34. Leung WH, Stadius ML, Alderman EL. Determinants of normal coronary artery
17	dimensions in humans. Circulation. 1991; 84:2294-2306.
18	35. Guo X, Liu Y, Kassab GS. Diameter-dependent axial prestretch of porcine coronary
19	arteries and veins. J Appl Physiol. 2012; 112:982-989.
20	36. Perry R, Joseph MX, Chew DP, Aylward PE, De Pasquale CG. Coronary artery wall
21	thickness of the left anterior descending artery using high resolution transthoracic
22	echocardiography-normal range of values. Echocardiography. 2013; 30:759-764.
23	37. Aidulis D, Pegg DE, Hunt CJ, Goffin YA, Vanderkelen A, van Hoeck B, et al. Processing
24	of ovine cardiac valve allografts: 1. Effects of preservation method on structure and
25	mechanical properties. Cell Tissue Bank. 2002; 3:79–89.

1	38. Goh KL, Chen Y, Chou SM, Listrat A, Bechet D, Wess TJ. Effects of frozen storage
2	temperature on the elasticity of tendons from a small murine model. Animal. 2010;
3	4:1613–1617.
4	39. Muller-Schweinitzer E. Cryopreservation of vascular tissues. Organogen. 2009; 5: 97-
5	104.
6	40. Burton HE, Williams RL, Espino DM. Effects of freezing, fixation and dehydration on
7	surface roughness properties of porcine left anterior descending coronary arteries.
8	Micron. 2017; 101: 78-86.
9	41. Thomas-Seale LEJ, Hollis L, Klatt D, Sack I, Roberts N, Pankaj P, Hoskins PR. The
10	simulation of magnetic resonance elastography through atherosclerosis. J Biomech. 49:
11	1781-1788.
12	42. Baxter J, Buchan KG, Espino DM. Viscoelastic properties of mitral valve leaflets: An
13	analysis of regional variation and frequency-dependency. Proc Inst Mech Eng Part H: J
14	Eng Med. 2017; 231: 938-944.
15	43. Lawless BM, Barnes SC, Espino DM, Shepherd DET. Viscoelastic properties of a spinal
16	posterior dynamic stabilisation device. J Mech Behav Biomed Mater. 2016; 59: 519-
17	526.
18	44. Sadeghi H, Espino DM, Shepherd DET. Variation in viscoelastic properties of bovine
19	articular cartilage below, up to and above healthy gait-relevant loading frequencies.
20	Proc Inst Mech Eng Part H: J Eng Med. 2015; 229: 115-123.
21	45. Constable M, Burton HE, Lawless BM, Gramigna V, Buchan KG, Espino DM. Effect of
22	glutaraldehyde based cross-linking on the viscoelasticity of mitral valve basal chordae
23	tendineae. Biomed Eng Online 2018; 17:93.
24	46. Abaqus version 6.10. Abaqus Analysis User's Manual; Part V: Materials. Dassault
25	Systemes Simulia Corporation. Providence, USA. 2010.